Thin-Walled Structures 84 (2014) 302–312

Contents lists available at ScienceDirect

Thin-Walled Structures

journal homepage: www.elsevier.com/locate/tws

Optimal shape design of thin-walled tubes under high-velocity axial impact loads

Niyazi Tanlak, Fazil O. Sonmez *

Department of Mechanical Engineering, Bogazici University, Istanbul, Bebek 34342, Turkey

ARTICLE INFO

Article history:
Received 2 October 2013
Received in revised form
7 July 2014
Accepted 7 July 2014

Keywords:
Thin-walled tubes
Crash-box
Crashworthiness
Explicit finite element analysis
Parametric system identification
Global optimization

ABSTRACT

In this study, the objective is to maximize the crashworthiness of thin-walled tubes under axial impact loads by shape optimization. As design variables, parameters defining the cross-sectional profile of the tube as well as parameters defining the longitudinal profile like the depths and lengths of the circumferential ribs and the taper angle are used. The methodology is applied to the design optimization of a crash-box supporting the bumper beam of a vehicle for the loading conditions in standard EuroNCAP crash tests. The crash event is simulated using explicit finite element method. While the crash-box is fully modeled, the structural response of the remaining parts during the tests is taken into account by developing a lumped-parameter model. A hybrid search algorithm combining Genetic and Nelder & Mead algorithms is developed. The results indicate significant improvement in the crashworthiness over the benchmarks designs.

1. Introduction

Thin-walled tubular structures are preferred in applications requiring high performance under impact loadings. In automobiles, thin-walled tubular parts are used to absorb impact energy in a potential crash. These parts should be designed to minimize the damage to the main parts of the vehicle and protect the occupants from injury by absorbing the collision energy. Their effectiveness in preventing injury under such impact loads is called crashworthiness. The performance of these parts can be significantly improved by optimizing their shapes.

There are a number of studies in the literature on the optimization of tubes made of metals (usually steel and aluminum) under axial impact loading. In these studies, tubes are considered as either empty [1–14] or filled [12,15–23]. Yamazaki and Han [1] studied square and cylindrical tubes hitting a rigid wall with a velocity of 10 m/s. They maximized the total energy absorption while maintaining the mean crushing force at a certain limit by varying the thickness of the tube and the section radius. Lee et al. [2] studied tubes with circular cross-section hitting a rigid wall with a velocity of 10 m/s and additional mass of 500 times the mass of the tube. Their design parameters were the wall thickness, radius, and length of the tube. Sheriff et al. [3] used the bottom diameter, height, and taper angle as design variables to maximize the total energy absorbed in circular cross-section tubes. Avalle and Chiandussi [4] optimized cylindrical tubes with tapered tip for uniform reaction force distribution. They varied the length of the tapered tip and the tip diameter. Hou et al. [5,6] optimized square and hexagonal single-cell and multi-cell tubes using base dimensions and thickness as design variables for minimum peak force and maximum specific energy absorption, i.e. energy absorption per unit mass. Acar et al. [8] varied taper angle and number of ribs on the surface in order to maximize the ratio of the mean crush force to the peak force and the specific energy absorption. Qi et al. [9] analyzed single and multi-cell square tubes under oblique impact. Their objective was to increase the specific energy absorption and minimize the peak crushing force by changing the taper angle and the wall thickness. Liu [10] optimized the wall thickness and the side length of a box-shaped column to maximize the specific energy absorption with a constraint on the peak force. Liu [11] considered straight and curved octagonal and hexagonal tubes and selected the side length and the wall thickness as variables. The objective was to maximize specific energy absorption of the columns while constraining the peak force. Yang and Qi [12] studied empty and filled tubes with a square cross-section under axial or oblique impact. Their objective was to increase the specific energy absorption and minimize the peak crushing force by varying the wall thickness, cross-section width, material yield strength, and filler material density. Zarei and Kröger [13] optimized empty cylindrical tubes by taking their length, diameter, and thickness as design variables for increased total energy and specific energy absorption. They extended that study to tubes filled with honeycomb [16] and foam [17] by considering their densities as variables. Kim and Arora [14] studied representation

* Corresponding author. Tel.: +90 212 359 7196; fax: +90 212 287 2456.
E-mail address: sonmezfa@boun.edu.tr (F.O. Sonmez).

http://dx.doi.org/10.1016/j.tws.2014.07.003
0263-8231/

of tapered tubes with uniform ones with square-sections in the force–displacement domain. With these force representations, a model with a single degree of freedom that simplified the analysis of the tube structure was identified. Santosa and Wierzbicki [15] studied the axial crushing resistance of a square-box column filled with aluminum honeycomb or foam under quasi-static loading conditions. Sun et al. [20] optimized crash-boxes with functionally graded foams for maximum specific energy absorption and minimum peak force. They assumed the foam material as layered and they varied the density of these layers. Hanssen et al. [18] used formulas derived based on experimental data relating design parameters to average force, maximum force, and stroke efficiency in order to obtain optimum designs of columns for minimum reaction force and maximum energy absorption. Ahmad and Thambiratnam [19] conducted a parametric study on empty and foam-filled tubes under axial impact loads using the wall thickness, taper angle, foam density, impact mass, and impact velocity as variables. Yin et al. [21] studied honeycomb-filled single and bitubular polygonal tubes. The variables were the wall thickness and the side length. The objective was to maximize the specific energy absorption and to minimize the peak force. Bi et al. [22] studied foam-filled single and multi-cell hexagonal tubes, which were crushed under a rigid wall moving downward with a velocity of 2 m/s and penetration depth of 100 mm. The variables were chosen to be the wall thickness and the side length of the section, and the foam density. The objective was to increase the specific energy absorption while keeping the mean crushing force larger than a certain limit to ensure a certain structural rigidity. Tarlochan et al. [23] conducted a parametric study on foam filled tubes under axial and oblique impact loading. They compared tubes having circular, square, hexagonal, octagonal, ellipsoidal cross-sections with the same circumference in terms of energy absorption and crush force efficiency.

The previous researchers generally developed approximate expressions for the objective functions using response surface methodology [1–6,8–11,13,16,17,20–22], Kriging [12], moving least-squares approximation [14], and artificial neural network [7]. After obtaining the surrogate models, they used genetic algorithms [3,16,17], leap-frog [7], particle swarm optimization [9,20,12,21], non-linear programming [5,6,8], or multi-first order method [4] as search algorithms.

The cross-sectional shapes of the tubes considered by the researchers were circular [1–4,8,13], square [1,5,7,9,10,12,16–20], hexagonal [6,11,21–23], or octagonal [11,21]. Some of the previous studies focused on straight columns with uniform cross-section along the length [1,2,5–7,9–13,16–18,20–22], some of them introduced taper angles [3,4,8,19], and some [8,7,16,17] introduced ribs with predefined shapes.

In the present study, a larger number of geometric parameters are used as optimization variables in comparison to the previous studies. The parameters defining the shape of the cross-sectional profile (the coordinates of key points defining the spline curves) and the longitudinal profile (depths and widths of the circumferential ribs, and the taper angle), and the wall thickness are varied. To the authors' knowledge, the shapes of the ribs are optimized for the first time in this study; in the previous studies, on the other hand, they were taken as constant. The ribs can be inward or outward. The taper angle can be positive or negative. Besides, the loading conditions considered in almost all the previous studies were either drop tests i.e. an object being dropped on a column, or a column with a mass at the rear hitting a rigid wall. In this study, the methodology developed for the optimum shape design of tubular structures is applied to the crash-boxes (or brackets) holding the bumper beam of a vehicle. The behavior of the crash-box is simulated for the loading conditions in a standard high-speed crash test, European New Car Assessment Program (EuroNCAP). Because of the difficulty in modeling the whole car and the resulting long computational times, a lumped-parameter car model is developed that accounts for the structural behavior of the main body of the vehicle as well as the parts in front of the crash-box. Moreover, in this study, a hybrid of genetic algorithm (GA) and Nelder–Mead algorithm is developed to find the globally optimal design or a near global optimal design.

The goal of global design optimization is to find the design with the best possible performance. This requires a definition of the geometric design that allows significant changes in shape, i.e. the solution domain should be large so that it includes the designs leading to the highest possible levels of performance. This means the number of geometric parameters and the range of values that can be assigned to these parameters by the search algorithm should be large. Global shape optimization of a vehicle for maximum crashworthiness is infeasible considering the high number of interacting parts, the high number of parameters used to define their geometries, and complex interactions among them during crash. This is beyond the capabilities of the current state-of the-art computers and search algorithms. Considering the computational effort to simulate crushing of the whole vehicle, it is not possible to find the globally optimum design within such a large solution domain and with such a large number of design variables even if a powerful global search algorithm is used. If large changes are allowed in the values of the optimization variables during optimization, the accuracy of surrogate models will also be questionable even for a single part let alone the whole vehicle. Besides, if the individual parts are separately optimized, loading conditions on them will be different from that of a drop test. That means the shape of a part optimized for the loading conditions in a drop test will not be optimum for the loading conditions in a real crash test.

The procedure suggested in this study to surmount these problems is the following: individual parts of the vehicle are optimized via a reliable global search algorithm by using a high number of design variables and allowing large changes in the values of these variables. The remaining parts of the vehicle are modeled with a system of lumped masses, springs, and dampers using parametric system identification, therefore computational times will not be prohibitively long. At the last stage, the whole vehicle is optimized starting from the optimized shapes of the individual parts, but this time the ranges of values that can be assigned to the variables will be small and some of the parameters may be taken as constant. Then, it becomes feasible to develop a reliable surrogate model for the vehicle and perform optimization. In this study, modeling and design optimization of a single part, a crash-box, is considered.

2. Problem statement

The main objective of this study is to develop a methodology to obtain the optimum shape design of thin-walled tubes subjected to high-velocity axial impact loads. The specific structure considered in this study is the bracket that supports the bumper beam of a car. Two brackets hold the bumper beam at two sides. They are in turn fixed to the main frame of the car. The types of obstacles that bumper-beam-crash-box system endures during frontal impact are countless. However, they can be categorized into three major divisions: full frontal collision, offset frontal collision, and pole frontal collision. The harshest collision that a bracket endures is the offset frontal impact, where one of the brackets takes the impact energy. Accordingly, the crash-box is optimized for offset collision conditions in accordance with EuroNCAP, IIHS, ANCAP standard tests, where the vehicle hits a wall with 40% offset and 64 km/h speed (See Fig. 1). At such high speeds, a car incurs substantial damage, but it is crucial that the occupants do not

suffer serious injury. Crashworthiness of the vehicle depends on the transferred impact force and the capacity of the structural parts to absorb the collision energy. The crash-box is one of the parts that should be optimally designed in order to achieve the required crashworthiness of the vehicle.

3. Approach

3.1. The objective function

The effectiveness of design optimization depends on the proper choice of the objective function. Improving its value should enhance the structural performance of the part in the most effective way. The following objective function is chosen to be maximized in the present study:

$$f_{obj} = \frac{w_1}{n_1}\frac{1}{\rho V}\int_0^{t_f}\iiint_V \sigma_{ij}\dot{\varepsilon}_{ij}\,dV\,dt - \frac{w_2}{n_2}\sqrt{\frac{1}{V}\iiint_V (\varepsilon-\bar{\varepsilon})^2\,dV} - w_3\left(\frac{1}{2n_{31}}F_{max}+\frac{1}{2n_{32}}\frac{F_{max}}{\Delta t}\right) - P \quad (1)$$

where V is the volume of the crash-box, t_f is the duration for which the simulation is conducted starting from the initial contact with the barrier, ε is the equivalent strain, $\bar{\varepsilon}$ is its mean value, F_{max} is the maximum force at the rear of the crash-box that occurs in the first 0.5 ms of the collision, and Δt is the time that passes until the maximum force occurs. The first term is the specific internal energy, or the energy absorbed per unit mass of the crash-box during crash. It is a measure of how effectively it takes the collision energy. The second term is a measure of uniformity in the deformation. This term is introduced to avoid shapes that result in highly localized deformation. The smaller this term is, the more uniform is the deformation; accordingly, the integrity of the tube is expected to be better maintained. The third term includes the magnitude of the peak force during the first 0.5 ms, F_{max}, as well as the average rate of increase in force, $F_{max}/\Delta t$. During collisions, generally the force transmitted reaches a peak value at the initial stages of the impact. It is essential to reduce the magnitude of the peak force as well as the rate of increase in force during the initial phases of the collision to reduce the jerking effect felt by the occupants during impact. w_i are the weighting constants, their values are chosen according to the relative importance that the designer gives to the individual terms, and n_i are the normalization constants, which are $n_1 = 38.1$ J/g, $n_2 = 1195$, $n_{31} = 156.7$ kN, and $n_{32} = 991.8$ MN/s. These values are obtained from the simulations conducted for a 70 mm diameter circular tube, which is taken as benchmark. P is the penalty function, which includes the following terms:

$$P = P_g + P_{mass} + P_{en} + P_{an} \quad (2)$$

P_g is the geometric constraint, which is activated when a cross-sectional profile generated by the search algorithm does not fit the allowable spacing. If P_g becomes active, a large value is added to the objective function without calculating the other terms. P_{mass} is the mass constraint such that

$$P_{mass} = \begin{cases} 0 & \text{if } m \le m_{ben} \\ 1000\left(\dfrac{m-m_{ben}}{m_{ben}}\right)^2 + 100\left(\dfrac{m-m_{ben}}{m_{ben}}\right) & \text{if } m > m_{ben} \end{cases}$$

where m is the mass of the crash-box and m_{ben} is the mass of the benchmark structure. The mass constraint is introduced in order to avoid optimal designs that show increased crashworthiness over the benchmark design at the expense of increased weight. P_{en} is the penalty introduced to eliminate the designs taking a lower impact energy in comparison to the benchmark case. Its value is calculated as

$$P_{en} = \begin{cases} 0 & \text{if } \bar{E}_{acc} \ge \bar{E}_{ben} \\ 3600\left(\dfrac{\bar{E}_{ben}-\bar{E}_{acc}}{\bar{E}_{ben}}\right)^2 + 450\left(\dfrac{\bar{E}_{ben}-\bar{E}_{acc}}{\bar{E}_{ben}}\right) & \text{if } \bar{E}_{acc} < \bar{E}_{ben} \end{cases}$$

where $\bar{E}_{acc}$ is the total accumulated energy in the crash-box and $\bar{E}_{ben}$ is the benchmark value for energy. P_{mass} and P_{en} are formulated such that the terms yield small penalty values for small violations, but the penalty value increases quadratically for large violations. P_{an} is the analysis constraint, which is activated when finite element analysis fails due to sharp corners or some other reason. By introducing the penalty terms, the constrained optimization problem is transformed into an unconstrained one.

The above metric is formulated to find the best shape that maximizes the specific energy absorption, avoids development of extreme plastic strains leading to rupture in the structure and also reduces the peak force and its jerk effect while ensuring that this is achieved by keeping the total energy absorption above certain limit without increasing the mass.

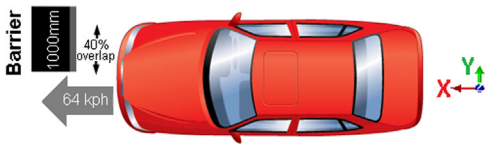

Fig. 1. A scheme for EuroNCAP frontal offset crash tests [24].

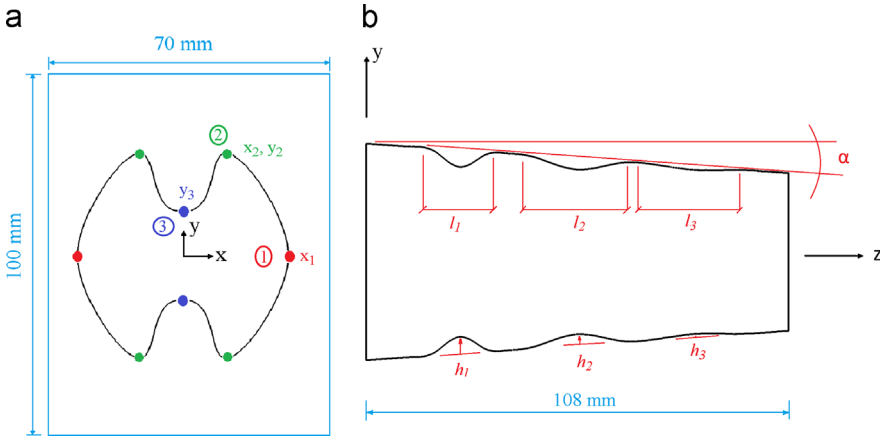

Fig. 2. Defining the cross-sectional (a) and the longitudinal (b) profile of the tube by spline curves.

3.2. The optimization variables and definition of the shape

In the present study, the shapes of both the cross-sectional profile and the longitudinal profile as well as the wall thickness of the crash-box are varied. Making use of the double symmetry of the cross section with respect to the x- and y-axes (Fig. 2a), only the shape of one-quarter is defined by a spline curve using three key points. Point 1 is allowed to move only horizontally; point 3 only vertically; on the other hand, point 2 can move in both directions. The longitudinal profile is defined by a series of coefficients as well as three length parameters. The first coefficient is the taper coefficient, c_α, which is used to define the taper angle, α. c_α is the ratio of the radial coordinates of the base and end-section key points. Furthermore, up to three ribs can be created at predefined locations along the crash-box. The profiles of the ribs are constructed using cubic spline curves, which are described by key points defined by depth coefficients, r_i, and length parameters, l_i (See Fig. 2b). $r_i \times c_\alpha$ is the ratio of the radial distance of the key point at the ith rib to that at the base. With the help of $r_i \times c_\alpha$, the depths of the ribs, h_i, are defined. The taper coefficient, c_α, can take values larger or smaller than 1.0. Accordingly, taper angle, α, can be positive or negative. Similarly, h_i may take positive or negative values; the ribs may then be inward or outward. Due to size limitations, constraints are imposed on the design variables such that the key points may not go outside the domain shown in Fig. 2a. In addition to the outer boundary of the design space, the key points defining the base cross-sectional profile are not allowed to enter the inner circular region with 12 mm radius in order to avoid numerical difficulties. The dimensions of the outer boundary are chosen based on the dimensions of a crash-box currently used in a Renault car. If the algorithm assigns a position for a key point outside this domain, a large penalty value, P_g, is assigned to the objective function.

3.3. Modeling the crash conditions

3.3.1. Modeling of the barrier

EuroNCAP uses a deformable barrier made of aluminum honeycomb in frontal offset-impact tests. The deformable barrier is designed to simulate an average collision partner during an accident. Although quite complex structural problems can be solved by FEM, analysis time should not be long in design optimization studies where thousands of runs may be needed to locate the globally optimum design or a near globally optimum design. For this reason, the barrier is modeled as rigid in the simulations. Because a rigid barrier does not absorb any impact energy, the effect of collision is severer. Deb et al. [25] used a lower velocity for the car in their simulations in order to account for the effect of deformable barrier. However, in this study, a lower mass is used for the car such that the severity of impact is more or less the same. The energy conservation equation for collision of a vehicle with a deformable barrier can be written as

$$\frac{1}{2}mv_0^2 = E_{vint} + E_{vke} + E_{bar} \tag{3}$$

where v_0 is the initial velocity of the vehicle, m is its original mass, E_{vint} is the energy absorbed by the vehicle, E_{vke} is the final kinetic energy of the vehicle after impact, and E_{bar} is the energy absorbed by the deformable barrier.

If the vehicle hits a rigid barrier with the same velocity, v_0, but with a different mass such that the same amount of energy, E_{vint}, is absorbed by the vehicle, then the equation becomes

$$\frac{1}{2}m'v_0^2 = E_{vint} + E'_{vke} \tag{4}$$

Here, m' is the equivalent vehicle mass and E'_{vke} is the final kinetic energy of the vehicle after impact. It now follows from Eqs. (3) and (4) that

$$m' = m - \frac{2}{v_0^2}(E_{bar} + E_{vke} - E'_{vke}) \tag{5}$$

Assuming $E_{vke} \approx E'_{vke}$, the above relation becomes

$$m' \approx m - \frac{2}{v_0^2}(E_{bar}) \tag{6}$$

According to Deb et al. [25], the ratio of the energy absorbed by the deformable barrier in a conventional offset test to the vehicle mass, E_{bar}/m, does not change much for cars of various masses. Taking E_{bar}/m as 82 J/kg as suggested by Deb et al. [25], m' is found to be 0.483 m, but to be on the safe side it is taken as 0.5 m. The mass of the vehicle is 1116 kg (904 kg $+2\times$ 88 kg$+$36 kg, which are the masses of Hybrid-III dummies of 88 kg and a luggage of 36 kg). So the effective mass, m', is 558 kg. In the simulations, the car hits a rigid wall with an initial velocity of 64 km/h (17.8 m/s) and 40% offset.

3.3.2. Modeling of the main vehicle body

Another concern is the modeling of the car. One option is to model the whole car as a deformable body in full detail, but this leads to excessively long computational times. Considering that a globally optimization procedure may require a high number of iterations, modeling the whole car is not a feasible option.

In this study, a lumped-parameter model is developed consisting of lumped masses, springs and dampers to account for the effects of the vehicle components behind the crash-box as well as the bumper beam in front of the crash-box, which is represented by a non-linear spring. Fig. 3 shows a depiction of the model used in this study. Because, at the early stages of the impact, plastic deformation mainly occurs in the bumper beam and the crash-box, then in the remaining structural parts of the vehicle, the main body is assumed to be linearly elastic and its mechanical response can be represented by linear springs during early phases of the collision during which the simulations are continued.

The model parameters are k_1, c_1, k_2, m_1, m_2, where k_1 and c_1 account for the elastic deformation and damping effects behind the crash-boxes, while the effect of the deforming bumper-beam is accounted for by a nonlinear spring. The force–displacement curve of this spring is defined by a quadratic polynomial, $F(u) = au^2 + bu$, up to $u = u^*$; after that the relation becomes linear, $F(u) = cu + d$. m_1 is the mass of the intermediary rigid plate and m_2 is the mass of the point mass such that $m_1 + m_2 = m'$. Here, the other crash-box is assumed to take no impact energy in offset impact tests.

In order for the lumped-parameter model to represent the behavior of the car during collision, suitable values for the model parameters should be chosen. For this purpose, the values of the model parameters are optimized so that the results of the present lumped-parameter car model match that of the full finite element

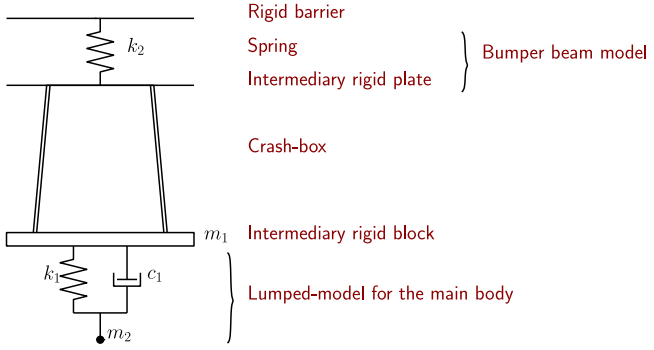

Fig. 3. A depiction of the vehicle model.

model for 2010 Toyota Yaris (Sedan), which was developed and validated by The National Crash Analysis Center (NCAC) of the U.S. [26]. This car model is crashed into a rigid wall with an offset according to the scenario specified above.

The lumped-parameter model is assembled with the crash-box as depicted in Fig. 3. Finite element simulations are conducted according to the collision scenario described above. The resulting reaction forces on the rigid barrier due to the collision are calculated as a function of time. The model parameters are optimized so that the impact forces on the wall obtained using the full car model and the lumped-parameter car model are as close to each other as possible. In order to estimate the closeness of the two outcomes, the following measure is used, which is the sum of the differences in the impact forces at corresponding time intervals:

$$f_{obj}=\sqrt{\sum_{i=0}^{100}\left[F\left(t_0+\frac{t_f-t_0}{100}i\right)-\tilde{F}\left(t_0+\frac{t_f-t_0}{100}i\right)\right]^2} \tag{7}$$

where t_0 is the initial time, t_f is the final time, F is the resulting impact force on the barrier for Toyota Yaris Model, and $\tilde{F}$ is the force for the lumped-parameter model. The values of k_1, c_1, m_1 together with the parameters defining the nonlinear spring representing the bumper-beam are optimized to yield the minimum value for f_{obj}. This optimization problem is solved using the same search algorithm used to optimize the crash-box. After optimizing the parameters, the force–displacement relation is obtained for the spring representing the bumper-beam.

As depicted in Fig. 4, the lumped-parameter model gives a response close to that of the full car model. The optimum values of parameters k_1, c_1, and m_1 are found to be 1690 10^6 N/m, 145.7 10^3 N s/m, and 112.79 kg, respectively. The parameters used to define the stiffness of the nonlinear spring are found to be $a=-2.9$ MN/m^2, $b=143.7$ MN/m, $c=1.4$ MN/m, $d=1.6$ MN and the transition displacement is obtained as $u^*=0.32$ mm.

3.4. Search algorithm

A search algorithm is utilized to find the optimum values of the variables that yield the maximum value for the objective function expressed in Eq. (1). Considering that typical structural optimization problems contain numerous local optimums, a local search algorithm may easily get stuck at a worse local optimum rather than the global optimum. If the problem has a complex solution domain, multiple restarts may even not work. Heuristic global search algorithms, on the other hand, may find the best configuration, but they require a large number of function calls for convergence. For this reason, they are not feasible for problems requiring long computational times like crash simulations. In the present study, in order to search for the globally optimum design without excessive computational burden, a hybrid algorithm combining global and local search algorithms is developed. In this method, the genetic algorithm (GA) is used to find configurations potentially close to the global optimum or one of the near global optimums. Then, these configurations are supplied to a local optimizer, Sequential Simples (Nelder & Mead) algorithm, which in turn locates the optimum.

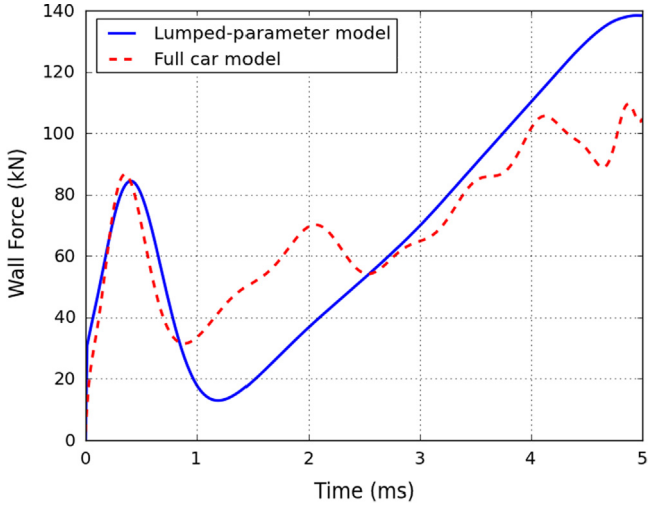

Fig. 4. Impact forces on the barrier resulting from car crash calculated using the lumped-parameter and the full car models.

3.5. Optimization procedure

In each iteration, new configurations are generated by the search algorithm. In order to evaluate the value of the objective function for these configurations, structural analyses of the corresponding crash events are carried out. For this purpose, a FE model is developed. The FE model and the optimization algorithm are integrated using a built-in ABAQUS python script. This code carries out FE analyses of the configurations generated by the search algorithm, writes the results on output files, and also evaluates the results to modify the values of the optimization variables according to the decision criteria of the hybrid search algorithm to obtain new candidate configurations.

At the start, the optimization code selects random values for the optimization variables within the feasible domain and creates the corresponding geometries of the crash-box. In this way, the initial population of GA is obtained. Using the predefined velocities, the boundary conditions, and the material properties, FE analyses are conducted for the randomly selected geometries. Based on the FE analysis results , the values of the objective function are calculated. The code then compares these values and selects new values for the optimization variables for the next generation according to the decision criteria of the GA. This procedure is repeated until the stopping criterion is satisfied, which requires no change in the best value found in three consecutive generations after the first 19 iterations. The initial population is taken as 300. The population is dynamic with an elitist approach that means it is initially high, but towards the end it gets lower; however the fittest member is always maintained. Crossover and mutation probabilities are also dynamic like the population. The best points found by GA are used as initial points by Nelder & Mead algorithm, which then tries to find the best local optimum in their neighborhood. Iterations are continued until the difference between the objective function values of the best and worst configurations becomes small.

4. Finite element modeling

Explicit FE methods are better in solving structural problems involving complex contact interactions occurring within a short duration compared to the implicit ones. Accordingly, commercial finite element software ABAQUS/Explicit is used in the present study to simulate the behavior of the crash-box system during crash tests.

4.1. Model geometry

The finite element model includes a deformable model of one crash-box as shown in Fig. 5. The main vehicle body is represented by a point mass, a spring, a damper, and an intermediary rigid block, which also serves uniform transmission of forces between the crash-box and the rest of the car. The bumper beam is

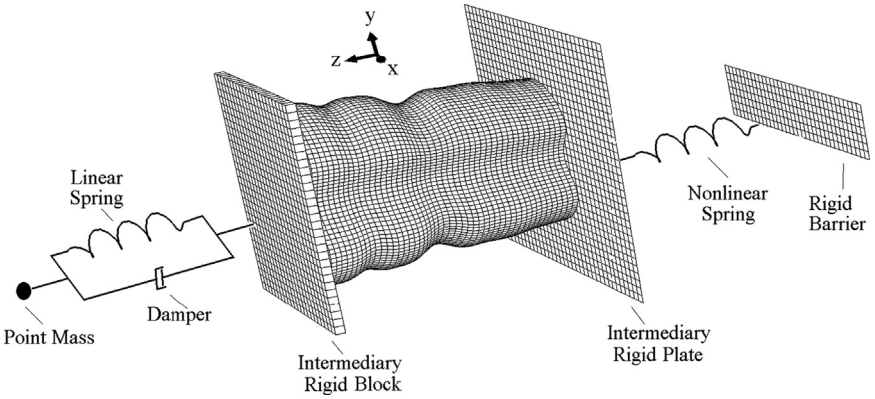

Fig. 5. Finite element model.

represented by a nonlinear spring, which is placed between the rigid plate and the rigid barrier for uniform force transmission.

4.2. Initial and boundary conditions

The initial and boundary conditions defined in the finite element model should reflect the conditions of the crash tests. Otherwise, the response of the crash-box cannot be correctly predicted. In the present finite element model, all parts except the rigid barrier have an initial velocity of 64 km/h (17.8 m/s). The rigid barrier which the car hits is fixed. The rear end of the crash-box and the intermediary rigid plate and block as well as the point mass are constrained to move only in the direction of the initial velocity so as to prevent relative movement of the blocks in the transverse directions considering that the transverse displacements are almost zero during the initial phases of the crash as shown in Fig. 6. Rotation of the vehicle occurs only at later stages of the crash. Because the geometry of the crash-box and the loading are symmetric with respect to the horizontal as well as vertical mid-planes, only one-quarter of the assembly is analyzed and the necessary symmetry conditions are applied on the corresponding interfaces.

4.3. Analysis time

Fig. 7 gives the energy absorbed by a circular crash-box, while Fig. 8 shows the change in the geometry of the crash-box at 1 ms intervals. As seen in the figures, the crash-box totally collapses after 5 ms, after that its stiffness greatly increases like a compression spring closed solid due to an overload, then a much larger energy is required to induce a small deformation. At this stage, the remaining portions of the car, which are initially stiffer than the bracket, start to absorb significant amount of energy. Accordingly, continuing the simulations longer than 5 ms is not appropriate, because the energy absorbing capacity of the bracket is consumed.

The analysis consists of a single explicit dynamic step. In the simulations, automatic time incrementation is used with element-by-element stable time increment estimates.

4.4. Constitutive model

Yield strength of materials typically increases with an increase in plastic strain as well as strain rate. During a crash test, the crash-box severely deforms in a very short time. For this reason, a realistic simulation of a crash event requires a constitutive model that accounts for non-linear and strain-rate dependent deformation and also work hardening. In the present FE model, Johnson–Cook constitutive model [27] is used. According to this model, the equivalent flow stress of the material, $\overline{\sigma}$, depends on equivalent

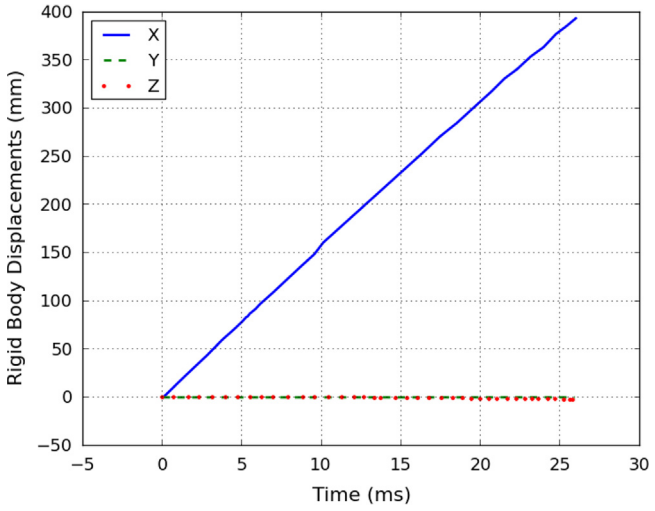

Fig. 6. Rigid body displacement history of Toyota Yaris model [26] during the initial stages of offset frontal impact.

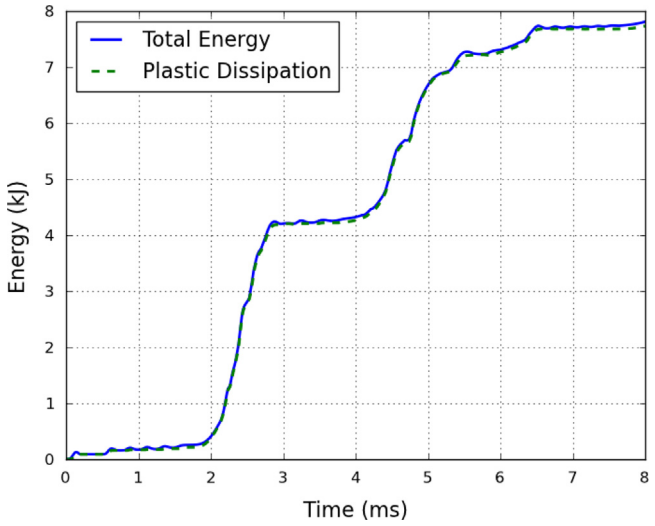

Fig. 7. Total energy values accumulated within a typical the crash-box during the collision.

plastic strain and its rate as

$$\overline{\sigma} = [\overline{\sigma_0} + B(\overline{\epsilon}^{pl})^n]\left[1 + C\ln\left(\frac{\dot{\overline{\epsilon}}^{pl}}{\dot{\epsilon}_0}\right)\right] \tag{8}$$

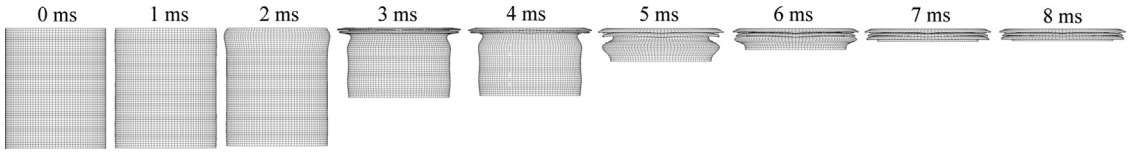

Fig. 8. Deformation of the crash-box with a circular base shape.

where $\overline{\epsilon}^{pl}$ is the equivalent plastic strain, $\dot{\overline{\epsilon}}^{pl}$ is its rate, $\dot{\epsilon}$ is the reference strain rate, and $\overline{\sigma_0}$ is the initial yield stress. The values of strain hardening coefficient, B, and exponent, n, can be obtained using quasi-static tension tests at the constant strain rate. The value of the strain rate parameter, C, is determined through dynamic tension tests conducted at different strain rates. Note that temperature effect is excluded in the present model.

4.5. Failure model

In crash tests, severe deformations are induced in the crash-box that can lead to local failures like cracks. Because failed elements may not continue to absorb energy, these may affect further deformation behavior and energy absorbing capacity of the crash-box. For this reason, a cumulative failure model proposed by Johnson and Cook [28] is adopted in this study.

In the model, a critical equivalent fracture strain, $\overline{\epsilon}_f^{pl}$, is defined, which depends on hydrostatic tension, p, and effective stress, $\overline{\sigma}$. The failure strain is expressed with four material constants, D_i, as

$$\overline{\epsilon}_f^{pl} = [D_1 + D_2 e^{D_3 \overline{\sigma}}]\left[1 + D_4 \ln\left(\frac{\dot{\overline{\epsilon}}^{pl}}{\dot{\epsilon}_0}\right)\right] \tag{9}$$

A damage parameter is defined as

$$\Omega = \frac{\overline{\epsilon}_0^{pl} + \sum \Delta \overline{\epsilon}^{pl}}{\overline{\epsilon}_f^{pl}} \tag{10}$$

where $\overline{\epsilon}_0^{pl}$ is the initial equivalent plastic strain and $\Delta\overline{\epsilon}^{pl}$ is an increment of the equivalent plastic strain. Ω is defined at the integration point of every finite element and is used as a measure of failure. Failure occurs when Ω exceeds the unity. If an element fails, very low values are assigned to the element for the mechanical properties.

4.6. Meshing

Considering that the thickness is small in comparison to the other dimensions, shell elements are used to model the walls of the crash-box. The element type used in the model is S4R, a 4-node quadrilateral shell element with reduced integration and a large-strain formulation. The elements account for both finite membrane strains and arbitrary large rotations. These elements allow transverse shear deformation. Thick shell theory is applied for thick shell elements while Kirchhoff theory is applied for thin shell elements. Simpson integration rule is used with five integration points through the thickness.

4.7. Contact modeling

The contact between the crash-box and the rigid plate and block is modeled using surface-to-surface contact modeling. However, in order to account for self-contact of the crash-box, the general contact algorithm is used in the finite element model. The value of the friction coefficient is chosen to be 0.15 for all the contact interactions.

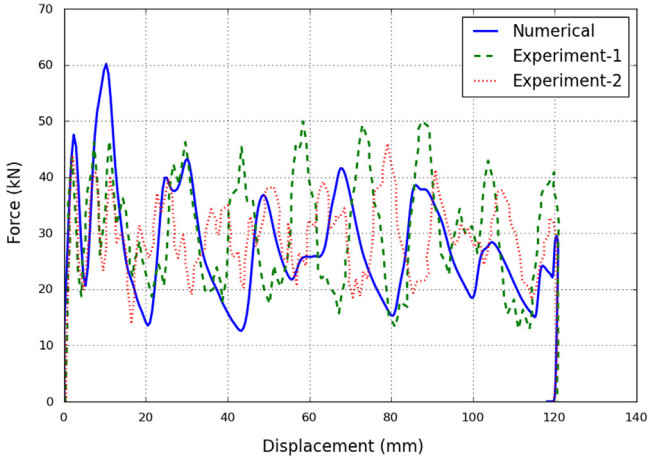

Fig. 9. Comparison of FEM results with the experimental drop test data [4].

5. Results and discussion

5.1. Comparison of FEM results with a test case

In order to validate the accuracy of the finite element model used in the present study, the model is adapted to a similar problem and the results obtained by the FE model are compared with the experimental results obtained by Avalle and Chiandussi [4]. The tests were conducted on a drop weight testing machine in which an object was dropped on a thin-walled tube with tapered tip at rest. The mass of the hammer was 60 kg and its initial velocity was 10 m/s.

The test is simulated using the aforementioned approach with an element size of 2.0 mm. Fig. 9 shows the relation between the force measured at the supports and the displacement measured. The numerical results correlate well with the experimental data as seen in Fig. 9.

5.2. Results of crash-box optimization

The shape optimization problem is solved using various combinations of weighting factors, w_i, in Eq. (1), either only one term in the objective function is used or more than one term, that means single and multi-objective optimizations are carried out. For single objective optimizations, the energy and mass constraints are not used. The optimization process is repeated for a constant thickness of 2.5 and 2.0 mm as well as variable thickness. The results are obtained for 6061-T6 aluminum alloy. The material properties provided by Corbett [29] are used in the simulations. The optimal shapes obtained by the algorithm and the optimal values of the optimization variables are given in Tables 1 and 2 respectively. Table 3 provides the results for the circular benchmark design. A comparison of the results for the optimum shapes as well as the chosen benchmark shapes is given in Table 4 in terms of the normalized values. Table 5 shows the deformation of the optimal crash-boxes during the course of collision.

It is noteworthy that the mass constraint ($m \leq 156$ g) and the total energy constraint ($\overline{E}_{acc} \geq 6672$ J) do not become active in the multi-objective optimizations except for the design obtained with

Table 1
Optimum base shapes of the crash-box for AL 6061-T6.

Weights	$t = 2.5$ mm	$t = 2.0$ mm	Variable t
$w_{1,2,3} = 1, 0, 0$	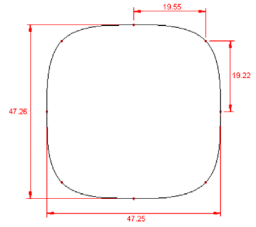	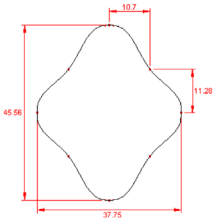	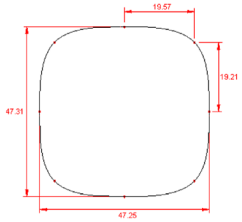
$w_{1,2,3} = 0, 1, 0$	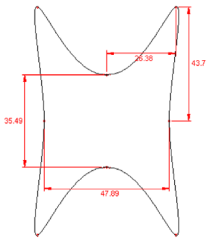	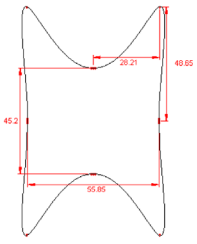	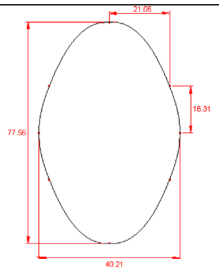
$w_{1,2,3} = 0, 0, 1$	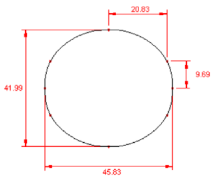	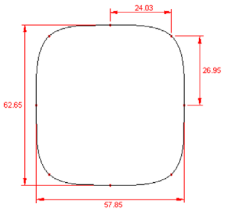	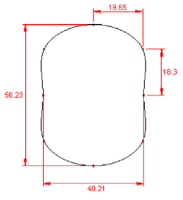
$w_{1,2,3} = 0.5, 0.1, 0.4$	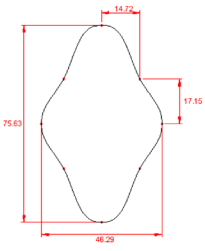	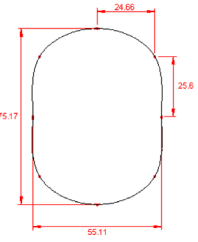	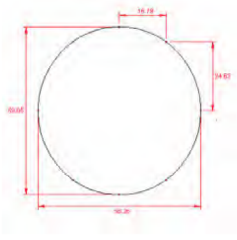
$w_{1,2,3} = 0.5, 0, 0.5$	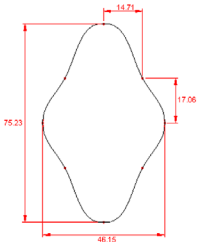	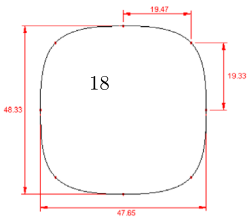	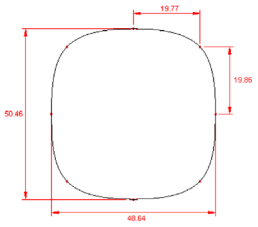

$w_{1,2,3} = 0.5, 0.1, 0.4$ and 2.0 mm thicknesses. In the single-objective optimizations, where the mass and energy constraints are not imposed, the masses of the optimal designs are also less than that of the circular crash-box except for the cases in which variance in the deformation is minimized with constant thickness. In contrast, if one tried to increase the static strength of the column, given the spacing limitations, one would increase the cross-sectional area, which would in turn decrease the stress. However, this would also increase its rigidity and thus reduce its capacity to absorb impact energy. In that case, the rest of the vehicle, which is represented by the lumped-parameter model in the present study, would take a significant portion of the impact energy. Too flexible columns, on the other hand, would quickly collapse and thus its energy absorbing capacity would be quickly consumed. One should recognize that simple rules of thumb will not work in complex problems. The optimization algorithm finds the optimal shapes that cannot be intuitively known because of the complexity of the deformation behavior.

The optimal shaped tube that can absorb the largest strain energy per unit mass is obtained if only the first term of the

Table 2
Optimal values of the optimization variables defining the longitudinal profile.

Weights	c_α	r_1	r_2	r_3	l_1 (mm)	l_2 (mm)	l_3 (mm)	t (mm)
$t=2.5$ mm								
$w_{1,2,3}=1,0,0$	0.8840	0.9902	0.9333	0.9879	20.0517	22.1671	19.7076	2.5
$w_{1,2,3}=0,1,0$	0.8931	0.8426	1.1138	0.8723	26.9095	15.3196	24.5560	2.5
$w_{1,2,3}=0,0,1$	1.4253	0.9691	0.8249	1.1216	15.7988	8.8586	17.1982	2.5
$w_{1,2,3}=0.5,0.1,0.4$	0.8616	0.8609	0.9859	1.0205	13.3882	17.5132	20.8555	2.5
$w_{1,2,3}=0.5,0.0,0.5$	0.8608	0.8610	0.9851	1.0203	13.3473	17.4272	20.9374	2.5
$t=2.0$ mm								
$w_{1,2,3}=1,0,0$	0.8294	0.9420	1.0167	1.0844	21.0814	18.4990	22.9199	2.0
$w_{1,2,3}=0,1,0$	0.7570	0.8798	1.1334	1.1106	10.0435	20.3362	7.5634	2.0
$w_{1,2,3}=0,0,1$	1.0776	1.0270	1.0406	0.8214	24.3266	9.0648	8.7931	2.0
$w_{1,2,3}=0.5,0.1,0.4$	1.1313	1.0274	1.0994	0.9873	14.6318	23.4376	28.3280	2.0
$w_{1,2,3}=0.5,0.0,0.5$	0.8895	0.9881	0.9318	0.9962	19.8434	22.5509	21.0224	2.0
Variable thickness								
$w_{1,2,3}=1,0,0$	0.8800	0.9854	0.9334	0.9892	20.0671	22.1775	19.6712	2.3721
$w_{1,2,3}=0,1,0$	0.7484	0.9715	0.9364	0.8969	17.6808	16.0072	12.2644	1.1077
$w_{1,2,3}=0,0,1$	1.2317	0.9108	0.8244	0.8841	24.3376	12.8680	14.1382	1.0143
$w_{1,2,3}=0.5,0.1,0.4$	0.8056	1.0007	0.9895	1.0589	17.0277	29.0038	27.0100	2.7044
$w_{1,2,3}=0.5,0.0,0.5$	0.9035	0.9946	0.9445	0.9995	19.6417	22.5352	21.2395	2.0195
Bench marks								
Circular ($D=70$)	1.0	1.0	1.0	1.0				2.5
Rectangular (70×100)	1.0	1.0	1.0	1.0				2.5

Table 3
Results for the circular benchmark design.

Weights	Specific energy (J/g)	Variance	F_{max} (kN)	$F_{max}/\Delta t$ (MN/s)	Mass (g)	Accumulated energy (J)
Circular ($D=70$)	42.8	1500	117.5	979.1	156	6672

Table 4
Comparison of the optimal and benchmark shapes in terms of normalized values.

Weights	Specific energy	Variance	F_{max}	$F_{max}/\Delta t$	Mass	Accumulated energy
$t=2.5$ mm						
$w_{1,2,3}=1,0,0$	1.61	4.79	0.83	0.53	0.72	1.16
$w_{1,2,3}=0,1,0$	0.41	0.56	0.95	0.81	1.46	0.59
$w_{1,2,3}=0,0,1$	1.02	1.48	0.51	0.12	0.85	0.86
$w_{1,2,3}=0.5,0.1,0.4$	1.45	1.85	0.68	0.39	0.82	1.19
$w_{1,2,3}=0.5,0.0,0.5$	1.46	1.98	0.68	0.39	0.82	1.19
$t=2.0$ mm						
$w_{1,2,3}=1,0,0$	1.63	3.71	0.46	0.29	0.44	0.71
$w_{1,2,3}=0,1,0$	0.45	0.46	0.87	0.50	1.23	0.56
$w_{1,2,3}=0,0,1$	0.87	0.65	0.31	0.08	0.87	0.76
$w_{1,2,3}=0.5,0.1,0.4$	1.11	1.64	0.54	0.32	0.90	1.00
$w_{1,2,3}=0.5,0.0,0.5$	1.57	5.94	0.84	0.52	0.72	1.13
Variable thickness						
$w_{1,2,3}=1,0,0$	2.34	5.85	0.77	0.47	0.67	1.56
$w_{1,2,3}=0,1,0$	0.66	0.29	0.17	0.10	0.36	0.24
$w_{1,2,3}=0,0,1$	0.72	0.31	0.10	0.02	0.36	0.26
$w_{1,2,3}=0.5,0.1,0.4$	1.33	1.91	0.89	0.73	0.85	1.12
$w_{1,2,3}=0.5,0.0,0.5$	1.80	4.37	0.64	0.39	0.59	1.06
Bench marks						
Circular ($D=70$)	1.0	1.0	1.0	1.0	1.0	1.0
Rectangular (70×100)	0.69	1.02	0.47	0.58	1.54	1.06

objective function is considered i.e. $w_1=1$, $w_2=0$, and $w_3=0$. Even though, in these runs, the third term, F_{max}, and $F_{max}/\Delta t$, is not considered, the resulting values are much better than that of the benchmark case. If only the second term is optimized, that means if the variance in the deformation is minimized ($w_1=0$, $w_2=1$ and $w_3=0$), unacceptably low specific energy values are obtained. If the third term in Eq. (1) is minimized ($w_1=0$, $w_2=0$, and $w_3=1$), the algorithm typically chooses larger taper angles and deeper circumferential ribs to minimize the jerk effect, but specific energy absorption is not improved. Besides, the total absorbed energies are much lower than that of the benchmark cases. When the three terms are considered with $w_1=0.5$, $w_2=0.1$, and $w_3=0.4$, more balanced results are obtained (Tables 1 and 5). Recognizing that the contribution of low variance in deformation to crashworthiness is questionable, the crash-box is optimized considering only the first and the third terms ($w_1=0.5$, $w_2=0$ and $w_3=0.5$). For this case, F_{max} and $F_{max}/\Delta t$ values are improved in comparison to the first case ($w_1=1$, $w_2=0$ and $w_3=0$). The crash-box designs with optimized thickness outperform the corresponding designs optimized using the same weights but with a predefined thickness.

Optimum design of the crash-box for high-speed collisions increases the crashworthiness of the vehicle, thus providing increased protection for passengers; however the crash-box must also satisfy the requirements for low-velocity impact so that it sustains limited deformation and prevents damage to the remaining parts of the vehicle. This requirement can be integrated to the optimization process in two ways. First, it can be used as a constraint, but this requires additional simulations of the low-velocity crash event at each iteration and thus significantly increases the computational times. Second, recognizing that many near global optimum designs are generated by the optimization process, in which the objective function values are very close, the optimization process is conducted without any regard for low-velocity impact performance, then the constraint is checked only for the optimal designs obtained at the end of the optimization process. Because it is more feasible and cost-effective, the second approach is adopted in this study. A standard low-velocity crash

Table 5
Comparison of the deformed shapes.

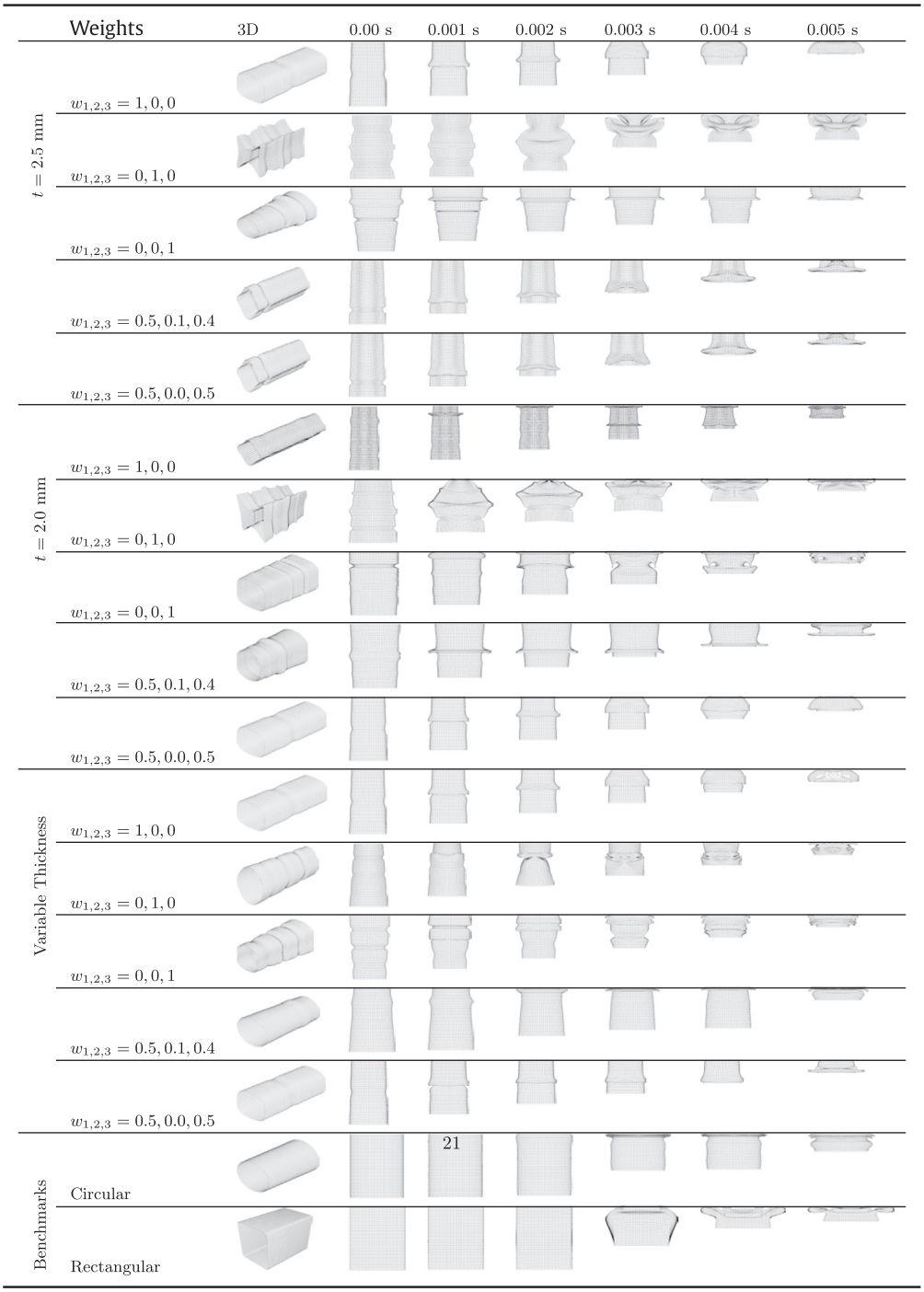

test, the Research Council for Automobile Repairs (RCAR) oblique frontal impact test, is used. In the RCAR test, a car with a velocity of 16 km/h hits a rigid wall oriented by 80° with respect to the direction of movement with 40% offset. The optimal designs presented in Table 2 and 4 as well as some near optimal designs are checked for low-velocity performance. Some of them are found to be better regarding low-velocity oblique impact requirements in comparison to the benchmark design, while some others are found to be worse. Table 6 gives a comparison of the performances of the circular benchmark design and the optimal designs of variable thickness having weights of $w_{1,2,3} = 1, 0, 0$ and $w_{1,2,3} = 0.5, 0.1, 0.4$. The optimal design of $w_{1,2,3} = 1, 0, 0$ shows a worse performance in comparison to the benchmark. On the other hand, the optimal design of $w_{1,2,3} = 0.5, 0.1, 0.4$ is better than the circular design in terms of specific energy absorption (SEA), F_{max} and F_{mean} and similar in performance in terms of accumulated energy and stroke efficiency, which is the displacement of the crash-box over its initial length. If the comparison is made for the circular design with the same mass, the performances of the optimal designs are far better in terms of energy absorption capability. In conclusion, one may state that optimizing a part for maximum crashworthiness does not ensure satisfaction of the low-velocity requirements, but one may find a design among the optimal designs that satisfies these requirements.

Table 6
Oblique impact results of selected designs.

Weights	SEA (J/g)	F_{max} (kN)	F_{mean} (kN)	Mass (g)	Stroke efficiency	Accumulated energy (J)
Circular ($D=70$; $t=2.5$ mm)	39.0	106.4	80.4	156	0.76	6081.3
Circular ($D=70$; $t=1.683$ mm)	27.2	59.8	31.6	105	0.83	2854.1
Circular ($D=70$; $t=2.15$ mm)	38.1	85.7	65.4	134	0.79	5106.8
$w_{1,2,3}=1,0,0$	37.0	70.5	47.3	105	0.92	3885.3
$w_{1,2,3}=0.5,0.1,0.4$	43.7	99.8	75.2	134	0.77	5859.4

6. Conclusion

In the present study, the shape of a crash-box is optimized under impact conditions very similar to EuroNCAP tests to maximize its crashworthiness. The parameters defining the shapes of the cross-sectional and longitudinal profiles as well as the thickness are taken as the optimization variables. The crash-box is modeled as a deformable body in full detail. In order to reduce the computational time, a lumped-parameter model is developed to mimic the behavior of the main vehicle body using a parametric system identification method. The parameters of the lumped-parameter car model are tuned to reflect the response of the car predicted by a full car model.

The resulting optimum shapes depend highly on the formation of the objective function, the number of variables, and the range of values that can be assigned to the variables. The optimum shapes obtained in this study show significant improvement over the benchmark designs. By choosing different values for the weighting factors of the terms in the objective function, different optimal shapes are obtained. The best results are obtained, if only the first and the third terms are considered. When the thickness is allowed to vary, the crashworthiness of the crash-box is improved.

The designs optimized for maximum crashworthiness at high-velocity impact may not satisfy low-velocity requirements, but it is possible to find near global optimums that show satisfactory performance for low-velocity impacts.

Acknowledgments

Scientific Research Projects of Bogazici University (Code number 5893) is gratefully acknowledged for supporting this research.

References

[1] Yamazaki K, Han J. Maximization of the crushing energy absorption of tubes. Struct Optim 1998;16:37–46.
[2] Lee S-H, Kim H-Y, Oh S-I. Cylindrical tube optimization using response surface method based on stochastic process. J Mater Process Tech 2002;130–131:490–496.
[3] Sheriff NM, Gupta NK, Velmurugan R, Shanmugapriyan N. Optimization of thin conical frusta for impact energy absorption. Thin-Walled Struct 2008;46:653–66.
[4] Avalle M, Chiandussi G. Optimisation of a vehicle energy absorbing steel component with experimental validation. Int J Impact Eng 2007;34:843–58.
[5] Hou S, Li Q, Long S, Yang X, Li W. Multiobjective optimization of multi-cell sections for the crashworthiness design. Int J Impact Eng 2008;35:1355–67.
[6] Hou S, Li Q, Long S, Yang X, Li W. Design optimization of regular hexagonal thin-walled columns with crashworthiness criteria. Finite Elem Anal Des 2007;43:555–65.
[7] Lönn D, Fyllingen O, Nilssona L. An approach to robust optimization of impact problems using random samples and meta-modelling. Int J Impact Eng 2010;37:723–34.
[8] Acar E, Guler MA, Gerceker B, Cerit ME, Bayram B. Multi-objective crashworthiness optimization of tapered thin-walled tubes with axisymmetric indentations. Thin-Walled Struct 2011;49(1):94–105.
[9] Qi C, Yang S, Dong F. Crushing analysis and multiobjective crashworthiness optimization of tapered square tube under oblique impact loading. Thin-Walled Struct 2012;59:103–19.
[10] Liu Y. Optimum design of straight thin-walled box section beams for crashworthiness analysis. Finite Elem Anal Des 2008;44:139–47.
[11] Liu Y. Crashworthiness design of multi-corner thin-walled columns. Thin-Walled Struct 2008;46:1329–37.
[12] Yang S, Qi C. Multiobjective optimization for empty and foam-filled square columns under oblique impact loading. Int J Impact Eng 2013;54:177–91.
[13] Zarei HR, Kröger M. Multiobjective crashworthiness optimization of circular aluminum tubes. Thin-Walled Struct 2006;44:301–8.
[14] Kim CH, Arora Jasbir S. Development of simplified dynamic models using optimization: application to crushed tubes. Comput Method Appl M 2003;192:2073–97.
[15] Santosa S, Wierzbicki T. Crash behavior of box columns filled with aluminum honeycomb or foam. Comput Struct 1998;68:343–67.
[16] Zarei HR, Kröger M. Optimum honeycomb filled crash absorber design. Mater Design 2008;29:193–204.
[17] Zarei HR, Kröger M. Optimization of the foam-filled aluminum tubes for crush box application. Thin-Walled Struct 2008;46:214–21.
[18] Hanssen AG, Langseth M, Hopperstad OS. Optimum design for energy absorption of square aluminium columns with aluminium foam filler. Int J Mech Sci 2001;43:153–76.
[19] Ahmad Z, Thambiratnam DP. Dynamic computer simulation and energy absorption of foam-filled conical tubes under axial impact loading. Comput Struct 2009;87:186–97.
[20] Sun G, Li G, Hou S, Zhou S, Li W, Li Q. Crashworthiness design for functionally graded foam-filled thin-walled structures. Mater Sci Eng A 2010;527:1911–9.
[21] Yin H, Wen G, Hou S, Chen K. Crushing analysis and multiobjective crashworthiness optimization of honeycomb-filled single and bitubular polygonal tubes. Mater Design 2011;32:4449–60.
[22] Bi J, Fang H, Wang Q, Ren X. Modeling and optimization of foam-filled thin-walled columns for crashworthiness designs. Finite Elem Anal Des 2010;46:698–709.
[23] Tarlochan F, Samer F, Hamouda AMS, Khalid K, Ramesh S. Design of thin wall structures for energy absorption applications: enhancement of crashworthiness due to axial and oblique impact forces. Thin-Walled Struct 2013;71:7–17.
[24] ⟨http://www.euroncap.com/tests/frontimpact.aspx⟩.
[25] Deb A, Naravane A, Chirwa EC. An offset rigid barrier-based test: equivalence to the insurance institute for highway safety frontal offset impact safety test. Int J Crashworthines 2006;11(4):281–90.
[26] ⟨http://www.ncac.gwu.edu/vml/models.html⟩.
[27] Johnson GR, Cook WH. A constitutive model and data for metals subjected to large strains, high strain rates, and high temperatures. In: Proceedings of the 7th international symposium ballistics; 1983.
[28] Johnson GR, Cook WH. Fracture characteristics of three metals subjected to various strains, strain rates, temperatures and pressures. Eng Fract Mech 1985;21(1):31–48.
[29] Corbett BM. Hypervelocity impact damage response and characterization of thin plate targets at elevated temperatures [Ph.D. thesis]. University of Denver; 2008.